

AD-A216 382

RADC-TR-89-214
Final Technical Report
October 1989



4

COMPUTER SIMULATION OF ELECTROMIGRATION IN THIN FILMS

Rensselaer Polytechnic Institute

H.B. Huntington, P.P. Meng, Y-T Shy

DTIC
ELECTE
JAN 03 1990
S B D

APPROVED FOR PUBLIC RELEASE; DISTRIBUTION UNLIMITED.

ROME AIR DEVELOPMENT CENTER
Air Force Systems Command
Griffiss Air Force Base, NY 13441-5700

00 01 03 054

This report has been reviewed by the RADC Public Affairs Division (PA) and is releasable to the National Technical Information Services (NTIS) At NTIS it will be releasable to the general public, including foreign nations.

RADC-TR-89-214 has been reviewed and is approved for publication.

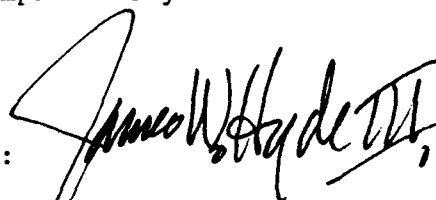
APPROVED: *M. W. Levi*

MARK W. LEVI
Project Engineer

APPROVED: *John J. Bart*

JOHN J. BART
Technical Director
Directorate of Reliability & Compatibility

FOR THE COMMANDER:



JAMES W. HYDE III
Directorate of Plans & Programs

If your address has changed or if you wish to be removed from the RADC mailing list, or if the addressee is no longer employed by your organization, please notify RADC (RBRP) Griffiss AFB NY 13441-5700. This will assist us in maintaining a current mailing list.

Do not return copies of this report unless contractual obligations or notices on a specific document require that it be returned.

REPORT DOCUMENTATION PAGE				Form Approved OMB No. 0704-0188	
1a. REPORT SECURITY CLASSIFICATION UNCLASSIFIED			1b. RESTRICTIVE MARKINGS N/A		
2a. SECURITY CLASSIFICATION AUTHORITY N/A			3. DISTRIBUTION / AVAILABILITY OF REPORT Approved for public release; Distribution unlimited.		
2b. DECLASSIFICATION / DOWNGRADING SCHEDULE N/A					
4. PERFORMING ORGANIZATION REPORT NUMBER(S) N/A			5. MONITORING ORGANIZATION REPORT NUMBER(S) RADC-TR-89-214		
6a. NAME OF PERFORMING ORGANIZATION Rensselaer Polytechnic Institute		6b. OFFICE SYMBOL (If applicable) RBRP	7a. NAME OF MONITORING ORGANIZATION Rome Air Development Center (RBRP)		
6c. ADDRESS (City, State, and ZIP Code) Dept of Physics Troy NY 12180-3590			7b. ADDRESS (City, State, and ZIP Code) Griffiss AFB NY 13441-5700		
8a. NAME OF FUNDING / SPONSORING ORGANIZATION Rome Air Development Center		8b. OFFICE SYMBOL (If applicable) RBRP	9. PROCUREMENT INSTRUMENT IDENTIFICATION NUMBER F30602-81-C-0193 Task #N-5759		
8c. ADDRESS (City, State, and ZIP Code) Griffiss AFB NY 13441-5700			10. SOURCE OF FUNDING NUMBERS	PROGRAM ELEMENT NO.	PROJECT NO.
11. TITLE (Include Security Classification) COMPUTER SIMULATION OF ELECTROMIGRATION IN THIN FILMS					
12. PERSONAL AUTHOR(S) H. B. Huntington, P. P. Meng, Y-T Shy					
13a. TYPE OF REPORT Final		13b. TIME COVERED FROM Nov 87 TO Oct 88		14. DATE OF REPORT (Year, Month, Day) October 1989	
15. PAGE COUNT 28					
16. SUPPLEMENTARY NOTATION N/A					
17. COSATI CODES			18. SUBJECT TERMS (Continue on reverse if necessary and identify by block number) Electromigration Modelling		
FIELD	GROUP	SUB-GROUP			
13	08				
19. ABSTRACT (Continue on reverse if necessary and identify by block number) Computational results of modelling electromigration in metal stripes without passivation but with reasonably realistic grain and grain-boundary configurations representing both unannealed and annealed stripes have shown moderate reductions in a measure of damage by electromigration in the annealed case.					
20. DISTRIBUTION / AVAILABILITY OF ABSTRACT <input checked="" type="checkbox"/> UNCLASSIFIED/UNLIMITED <input type="checkbox"/> SAME AS RPT. <input type="checkbox"/> DTIC USERS			21. ABSTRACT SECURITY CLASSIFICATION UNCLASSIFIED		
22a. NAME OF RESPONSIBLE INDIVIDUAL Mark W. Levi			22b. TELEPHONE (Include Area Code) (315) 330-2075		22c. OFFICE SYMBOL RADC (RBRP)

EVALUATION

This work has shown a computational and modelling of electromigration in annealed and unannealed metal stripes which is consistent with the experimental literature observation that annealed, and consequently larger grained, films tend to have longer lives than do unannealed films. Modelling successes such as this are essential to a complete understanding of this life-limiting process.

M. W. Levi
Mark W. Levi



Accession For	
NTIS GRA&I	<input checked="checked" type="checkbox"/>
DTIC TAB	<input type="checkbox"/>
Unannounced	<input type="checkbox"/>
Justification	
By	
Distribution/	
Availability Codes	
Dist	Avail and/or Special
A-1	

I. Introduction and Review

A. Relation to other computer simulation projects

There have been several past and current computer simulations of stripe damage caused by electromigration, some of which were listed in the references accompanying my original proposal. Most of these programs have been run many times to afford statistical information on the half-life to failure and the corresponding random spread parameter. Thereby they have been able to afford considerable valuable information on the influence of grain size and of stripe dimension and, in an approximate way, to take into account the effects caused by current and temperature inhomogeneities.

Our project differs from these other simulations in two respects: (1) we have tried to make our model somewhat more realistic and detailed and (2), as a consequence of the increased complexity, we shall probably be limited to only those initial stages of damage before the effects of current and temperature inhomogeneities become important. Although well developed statistical results will be difficult to come by, we can explore the influence of texture, annealing and surface condition on damage by electromigration. The approach should provide a useful alternative to other computer simulations.

B. Review of prior results in this area:

The initial work in setting up this project was concerned with developing a suitable two-dimensional network to simulate the $\{111\}$ texture of the metallized stripe. For this a Voronoi procedure was applied and the grains of the structure were assigned random orientations. The grain boundary behavior followed the dislocation model for misorientation angles less than 32° and was assumed to be isotropic for greater misorientations. On the basis of this model expressions were developed for both the grain boundary diffusivities and the grain boundary tensions.

The next step was to relax the grain boundary tensions by displacing the network vertices appropriately. In Figs. 1 and 3 we show Voronoi pattern for a wide stripe A (15 μm) and a medium stripe B (10 μm). In adjoining Figs. 2 and 4 are shown the same stripes after equilibration of g.b. forces. This process could be thought of as a form of annealing. It has bearing on the electromigration damage process in that the condition for stress relaxation by vertex motion along the axis parallel to the current is closely related to the equation for mass accumulation (or deficit) at the vertex in question.

In proceeding now to the actual electromigration one writes out the diffusion equation appropriate to conditions of forced motion from electromigration. Working toward a solution of this equation leads to two approximations:

1. Because the time constant of the network segments (L^2/D) were so short, it was reasonable to bypass the transient solutions and move directly to steady-state, or quasi steady-state, solutions.
2. It became apparent that the principal effect of the electromigration on the mass distribution in the grain boundaries came about directly at the vertices and its effect secondarily on the concentration distributions in the segments was small. Accordingly the electromigration term in the diffusion equation was dropped and only considered right at the vertices.

At each vertex one evaluates $F_v = \sum_{\sigma} D_{\sigma} A_{\sigma} \cos \phi_{\sigma} M_0$ where the summation is over the various segments that meet at the vertex, D_{σ} is the diffusion coefficient for each segment as determined by the misorientation between the grains on either side of the grain boundary, and the angles ϕ_{σ} are between the direction of the grain boundary and the electric current. The number of atoms per unit length of grain boundary is M_0 . The constant A_0 is $|e|Z^*E/kT$ where

e is the electron charge, E the electric field and T the temperature. Z^* is the effective charge number for electromigration which is around -20 for aluminum. If $F_v < 0$, the vertex is a deficit vertex (-) and conversely if $F_v > 0$, the vertex is an excess vertex (+).

The (+) or (-) vertices are treated quite differently. The net deficit at the (-) vertices is considered to contribute directly to a growing, circular cylindrical void. At the (+) vertices the matter can not pile up at a point but must diffuse back along the grain boundaries. As a result the (--) segments maintain the uniform grain boundary concentration according to our model. For the (+-) segments the concentration goes to zero at the (-) end but may build up at the (+) end. There is build-up at both ends of the (++) segments.

We have been concerned with electromigration under two extreme surface conditions: free surface and the surface covered with a passivating layer which prevents flow up out the grain boundary. These two situations will be discussed respectively in the next two sections.

II. Electromigration under the Free Surface

According to the model the excess material from the (+) vertices diffuses down the grain boundaries and up out of the grain boundaries to cover the surface quite smoothly. This situation can be expressed mathematically simply by solutions which are steady state within the grain boundaries. The solutions must satisfy the Laplacian and will be of the form \cosh (or \sinh) $\gamma x \cos \frac{\pi z}{2d}$ where x is measured along the g.b. and z is measured from the substrate to the free surface. Accordingly the surface deposits centered at the (+) vertices grow with time as do the voids centered at the (-) vertices.

We summarize the mathematical treatment next, starting with the differential equation for mass movement,

$$\frac{\partial M_{\sigma}(x,z,t)}{\partial t} = \frac{\partial}{\partial x} \{ D_{\sigma\perp} \left[\frac{\partial M_{\sigma}(x,z,t)}{\partial x} - A M_{\sigma}(x,z,t) \right] \} + \frac{\partial}{\partial z} \{ D_{\sigma\parallel} \frac{\partial M_{\sigma}(x,z,t)}{\partial z} \} \quad (1)$$

where $M_{\sigma}(x,z,t)$ is the amount of material in the σ -grain boundary per unit length (x) of boundary. The z is measured perpendicular to the surface from the substrate to the free surface. The subscript σ denotes the segment under consideration. $D_{\sigma\perp}$ means the diffusion coefficient perpendicular to the dislocations in the grain boundary, i.e. along the surface, and $D_{\sigma\parallel}$ is for motion parallel to the dislocations, i.e. at right angles to the substrate.

Let us write

$$M_{\sigma}(x,z,t) = M_0 + m(x,z,t) \quad (2)$$

where M_0 is the equilibrium number of atoms per unit length of grain boundary, or $N\delta d$ where N is the number of atoms per unit volume, d is the thickness of the stripe and δ is the width of the grain boundary or roughly one atom dimension. The grain boundary segments can be categorized by the nature of their end points, $(--)$, $(+-)$ and $(++)$. Because of void formation there is no back diffusion long the $(--)$ segments and $m_{\sigma} = 0$. For the other segments we are interested in the time independent situation after the transient,

$$m(x,z,\infty) = m_{\sigma}(x) \frac{\pi}{2d} \cos(\pi z/2d) \quad (3)$$

The form of the z -dependence is chosen to give all matter flow at the surface and none at the substrate. The equation for $m(x)$ now becomes

$$m''(x) - A_{\sigma} m'(x) - C m(x) = 0 \quad (4)$$

$$\text{with solutions } m(x) = a e^{\gamma_1 x} + a e^{\gamma_2 (x-L)} \quad \text{where} \quad (5)$$

$$\gamma_{1,2} = \frac{A_{\sigma}}{2} \pm \left(\left(\frac{A_{\sigma}}{2} \right)^2 + C \right)^{\frac{1}{2}} \quad \text{and} \quad C = \frac{D_{\sigma\parallel}}{D_{\sigma\perp}} \left(\frac{\pi^2}{2d} \right) \quad (6)$$

Since $D_{\parallel} > D_{\perp}$ in every case and $d \sim 1\mu$ while $A \sim 0.1\mu$, $A/2$ is usually much smaller than $C^{\frac{1}{2}}$ so that $\gamma_1 \approx -\gamma_2 = -\gamma$. This is consistent with our second approximation as stated earlier.

We concentrate now at one vertex m_v and consider in turn each connecting segment as indexed by σ . For each segment there are two equations, taking $x = 0$ at the vertex in question.

$$m_v = a_1 + a_2 e^{-\gamma L} \quad (7)$$

$$m_{v\sigma} = a_1 e^{-\gamma L} + a_2,$$

where $m_{v\sigma}$ is the value of m at the other end of the σ -segment. For the (+) segments $m_{v\sigma} = 0$, $a_2 = -a_1 e^{-\gamma L}$ and $m_v = a_1 (1 - e^{-2\gamma L})$.

The magnitudes of the m_v , or a 's are determined by the condition at the (+) vertices that the diffusion flux carries away the excess material deposited by electromigration

$$F_v = - \sum_{\sigma} D_{\sigma\perp} \left(\frac{\partial m_{\sigma}}{\partial x} \right). \quad (8)$$

Based on eq. (5).

$$\left[\frac{\partial m_{\sigma}}{\partial x} \right]_v = -\gamma a_1 + \gamma a_2 e^{-\gamma L} \quad (9)$$

but

$$a_1 = (m_v - e^{-\gamma L} m_{v\sigma}) (1 - e^{-2\gamma L})^{-1} \quad (10)$$

$$a_2 = (m_{v\sigma} - e^{-\gamma L} m_v) (1 - e^{-2\gamma L})^{-1}$$

Hence

$$F_v = \sum_{\sigma} D_{\sigma\perp} \gamma_{\sigma} (m_v (1 + e^{-2\gamma L}) - 2e^{-\gamma L} m_{v\sigma}) (1 - e^{-2\gamma L})^{-1} \quad (11)$$

We now solve for m_v

$$m_v = [F_v (1 - e^{-2\gamma L}) + \sum_{\sigma} 2e^{-\gamma L} D_{\sigma\perp} \gamma_{\sigma} m_{v\sigma}] / \sum_{\sigma} D_{\sigma\perp} \gamma_{\sigma} (1 + e^{-2\gamma L}) \quad (12)$$

To solve equations 12 there is the initial difficulty that the $m_{v\sigma}$ are unknown. This can be overcome by iteration on the computer. Let the index n designate the m value at the end of the n th stage of iteration.

$$m_{v(n+1)} = [F_v (1 - e^{-2\gamma L}) + \sum_{\sigma} 2e^{-\gamma L} D_{\sigma\perp} \gamma_{\sigma} m_{v\sigma n}] / \sum_{\sigma} D_{\sigma\perp} \gamma_{\sigma} (1 + e^{-2\gamma L}) \quad (12a)$$

We begin the first step with $m_{v\sigma 0} = 0$.

In the course of each step in the iteration process there will be occasion to note for the (+) segments a rate of deposit at the (-) ends of $2D_{\sigma\perp} \gamma_{\sigma} \exp(-\gamma_{\sigma} L_{\sigma}) / (1 - e^{-2\gamma_{\sigma} L_{\sigma}})$ which tends to compensate the deficit caused by the original $F_v < 0$. We represent the missing material by circular cylinder.

$$NV_d = N\pi R^2 d = -t \{ F_v + \sum_{\sigma} [2m_{\sigma} D_{\sigma\perp} \gamma_{\sigma} e^{-\gamma_{\sigma} L_{\sigma}} / (1 - e^{-2\gamma_{\sigma} L_{\sigma}})] \} \quad (13)$$

If the quantity inside the { } turns positive, the vertex changes from (-) to (+) and must be so considered + in subsequent iterations with $F_v' = \{ \}$.

The result of this electromigration under a free surface is illustrated by Figs. 5-8.

The technique we have employed is to represent the deficit cylinders by

open circles scaled to size and the build-up regions by cross hatchings whose amplitudes are in proportion to the excess material in the grain boundaries. There was a need to choose an index to measure the extent of damage for each stripe. For this we took f_c , the fraction of stripe volume converted to void by the electromigration action. The f_c - values for Stripes A & B before and after equilibration are given in Table I. Note the extent to which equilibration has improved stripe resistance to electromigration damage.

III. Electromigration Under a Passivating Layer

This situation is just the opposite extreme from that of the free surface treated in the preceding section. Any escape of the material in the grain boundary to the surface is prevented by the passivation. The pressures in the grain boundaries connected to excess vertices thereby increase to limiting values, assuming no rupture of the passivation. This eventually attained steady state occurs when the electromigration influx at any excess vertex is balanced by the outward flow to nearby (weaker) excess vertices or to deficit vertices.

The build-up period described above has proved very difficult to model satisfactorily. We have made several attempts which have failed. Currently we have developed an approach which looks promising, but testing with a suitable program has been delayed as a new programmer is learning the ropes.

This approach is built around the use of a particular function which is a solution of the diffusion equation in the segments.

$$C(x,t) = (x/L)^2 + 6D \frac{x}{L^3} t = (x/L)^2 + 6 \frac{x}{L} (t/\tau_r) \quad (II,1)$$

where L , D and τ are respectively the segment length, the diffusivity in the segment and the segment time constant $\tau_0 = D_0/L_0^2$. Accordingly we start the build-up timing after a short transient period and assume that the

m-distribution in the (+ -) segments is given by

$$m_{\sigma}(x,t) = \mu_{\sigma}(t) C_{\sigma}(x,t) \quad (II,2a)$$

and in the (++) segments by

$$m_{\sigma}(x,t) = \mu_L(t) C_{\sigma}\{(L-x), t\} + \mu_R C_{\sigma}(x,t) \quad (II,2b)$$

where subscripts L and R refer to the right and left ends of the segment and the μ are presumably slowly varying functions of time. The presence of the μ 's does of course prevent the m functions from being solutions of the diffusion equation, particularly as the function of the μ is to bring the m's to steady state values and to stop the linear increase with time. We believe, however, that this is not a serious weakness, since one can devise a solution which is a series of functions, dominated by a first term which saturates. It remains now to invoke the condition established for the F_v .

$$F_v = \sum_{\sigma}^{+ -} \frac{D_{\sigma}}{L_{\sigma}} (3 + 6 \frac{t}{\tau_{\sigma}}) \mu_v(t) + \sum_{\sigma}^{++} [\frac{D_{\sigma}}{L_{\sigma}} [3 \mu_{v\sigma} + \frac{6t}{\tau_{\sigma}} (\mu_v - \mu_{v\sigma})]] \quad (II,3)$$

At the end of the transient ($t = 0$)

$$\mu_v^{(0)} = m_v(0) = F_v / \sum_{\sigma} 3 (D/L_{\sigma}) \quad (II,4)$$

After a short interval, Δt ,

$$\mu_v(\Delta t) = \{F_v + \sum_{\sigma}^{++} \{D/L_{\sigma} (\Delta t/\tau_{\sigma}) \mu_{v\sigma}\} / \sum_{\sigma} (D/L_{\sigma}) (3 + \frac{6(\Delta t)}{\tau_{\sigma}})\} \quad (II,5)$$

Here the $\mu_{v\sigma}$ are the μ -values on the (+) vertices which are linked to vertex v. For them we approximate with $\mu_{v\sigma}(0) = m_v(0)$ initially. It may be advisable to follow later with one stage of iteration, using Eq. II, 5 a second time with the $\mu_{v\sigma}^{(1)}(\Delta t)$ on the right hand side to get improved $\mu_v(\Delta t)$. For succeeding time steps it should be sufficient to extrapolate

$$\mu_{v\sigma}^{[n + \frac{1}{2}]} = 1/2 [\mu_{v\sigma}^n - \mu_{v\sigma}^{n-1}] + \mu_{v\sigma}^n \quad (II,6)$$

to be used in the extension of (II, 5) to long times.

Obtaining m_v , now that the μ_v are determined, runs into a difficulty with the C-functions as introduced in (II, 2). Our method insures that the μ_v is a function of v only but this is not true of C_σ where one sees a σ dependence in the (t/τ_σ) . To bypass this difficulty we replace $\frac{1}{\tau_\sigma}$ by $\frac{1}{\tau_v} = \frac{3}{3} \sum_{\sigma} \frac{1}{\tau_\sigma}$.

With the use of this crude approximation we can now write

$$m_v(t) = \mu_v(t) \{1 + 6 t/\tau_v\} \quad (II,7)$$

At each step in the time progression one must also calculate the m_v from II, 2 and also the spill-over at the $(-)$ vertices. For these vertices the void volume, Ω_v , is given by

$$\Omega_v(t_n) = \sum_{n=1}^n \left\{ - \sum_{\sigma}^{+-} \mu_{v\sigma} 6(t_n'/\tau_\sigma) - F_v \right\} (\Delta t)_n' \quad (II,8)$$

where $t_n' = \sum_{1}^n (\Delta t)_n'$ and $F < 0$ for $(-)$ vertices

The first term in the curly brackets comes from the spill-over effect (S-0). If the S-0 term becomes bigger than $-F_v$ the void may fill up. If this happens, the program should recognize that the vertex has changed from $(-)$ to $(+)$ with an effective $F_v' = - \{ \quad \}$ of equation (II 7). It will be important to get some measure of the extent to which the original number of voids is reduced by this filling process.

What form will the m_v take at long time?

One can obtain from Eq. II 5 a set of linear relations for

$$m_v(\infty) = \lim_{\tau \rightarrow \infty} 6\mu_v(t) t/\tau_v \text{ as defined by Eq. II 7}$$

These relations are

$$m_v(\infty) \sum_{\sigma} (D/L)_{\sigma} = F_v + \sum_{\sigma}^{++} (D/L)_{\sigma} m_{v\sigma}(\infty) \quad (II,9)$$

by transforming Eq. (II 5). This shows that it is possible to obtain the final values for m_v without following through the detailed development in time. A method of checking the detailed treatment is thereby provided.

This procedure appears promising in that it seems to have avoided the singularities and divergencies which wrecked earlier attempts at developing a treatment of the passivated layer case. Actual implementation is, however, held up temporarily while a new programmer is learning the operation of the project.

IV. Future Plans (from Jan. 1988 report)

1. If the procedure outlined in the previous section works well for the strongly passivated stripe, we should learn how long it takes to reach the steady state and at what build-up levels, what fraction of the voids become filled and what the influence of stripe dimensions and stripe annealing might be. For a truly realistic picture one needs to make provision for the rupture of the passivity layer and the formation of a hillock. Presumably this will occur at a predetermined stress level or perhaps value of m_v . From there on out m_v at this vertex is zero. The F_v from electromigration goes directly to increasing the "whisker" and has no effect on, $m(x)$. Likewise now the diffusional flux is inward at the vertex in question and the general tendency for void formation in the neighborhood is increased, as has been observed experimentally. This occurs mainly because of the reduction in "spill-over".
2. We also want to explore the effect of surface electromigration which will cause void motion in the opposite direction from the mass motion. For simplicity we take the void cylinders to be initially circular and assume that surface diffusion maintains this shape as that of minimum surface energy. The mass transport from one half of the void surface to the other is given by $2D_s A_0 d$ as calculated at those surface elements of the void parallel to the

current. Here D_s is the surface diffusion coefficient. Dividing the transport by the number of atoms missing in the void gives the void velocity, v_c .

$$v_c = 2D_s A_o / N\pi R^2$$

Apparently the smaller voids move more rapidly and so tend to catch up and coalesce with the larger voids. The process of surface electromigration also tends to distort the cylinders into cracks along the grain boundaries, a feature that may be difficult to simulate. Nevertheless it may be quite important in the deterioration process.

3. Another feature which we plan to consider is the possibility of invoking grain growth more directly in the annealing process than results from the stress equilibration process. This would be done by looking for those grains which may disappear altogether as a result of surface tension.

4. One interesting ramification of the above might arise if one postulates as a result more rapid grain growth on the surface of the stripe than at the stripe-substrate interface. As a consequence not all grain boundaries will be perpendicular to the stripe surfaces. Then some of the voids may not be right circular cylinders but develop "end" sections across which rapid surface electromigration can occur. This effect could contribute very substantially to void motion, but would involve 3-dimensional consideration which would introduce formidable complications.

5. On the other hand the treatment of peaked electromigration (or even ac operation) appears straightforward and perhaps well worth pursuing.

The numerous effects and responses of a stripe undergoing electromigration are so dramatic and varied that it is unrealistic to hope to incorporate them all in a single simulation. We have tried in this section to propose only a few aspects of the general problem which evolve from the particular model we have devised and are therefore susceptible to investigation in future studies.

Table I Values of f_c

	<u>Original</u>	<u>After Equilibration</u>	<u>Ratio</u>	
Stripe A	3.70%	2.07%	.56	.
Stripe B	3.27%	2.16%	.66	

List of Figure Captions

1. Wide stripe A - Voronoi construction
2. Wide stripe A after equilibration
3. Stripe B - Voronoi construction
4. Stripe B after equilibration
5. Effect of electromigration on Stripe A - before equilibration
6. Effect of electromigration on Stripe A - after equilibration
7. Electromigration on Stripe B - before equilibration
8. Electromigration on Stripe B - after equilibration

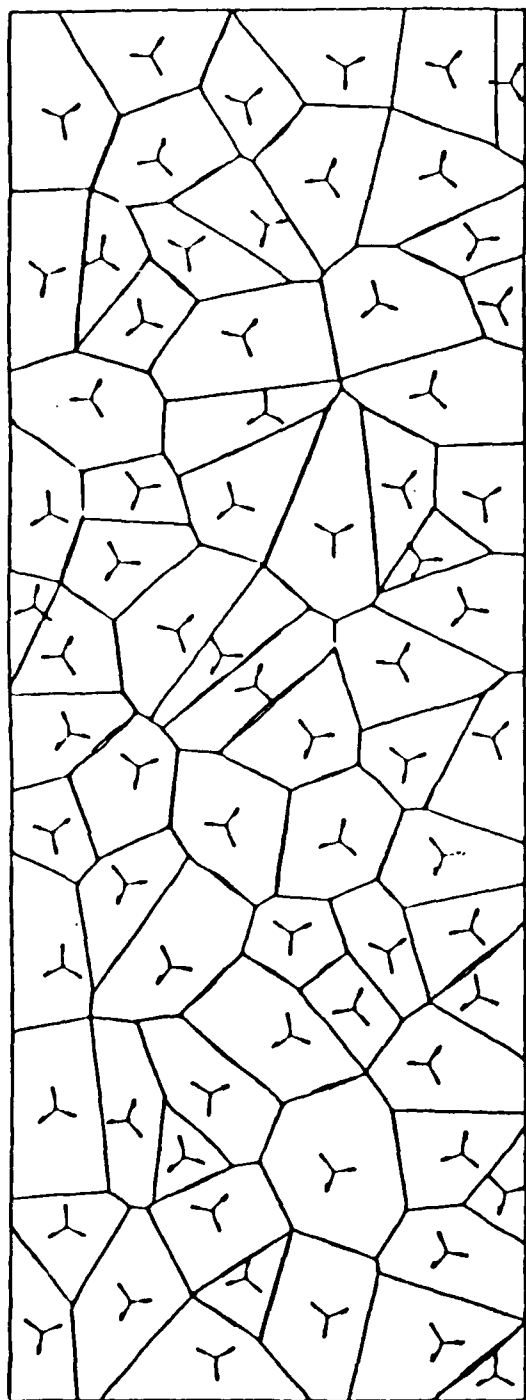


Figure 1 - Wide stripe A - Voronoi construction

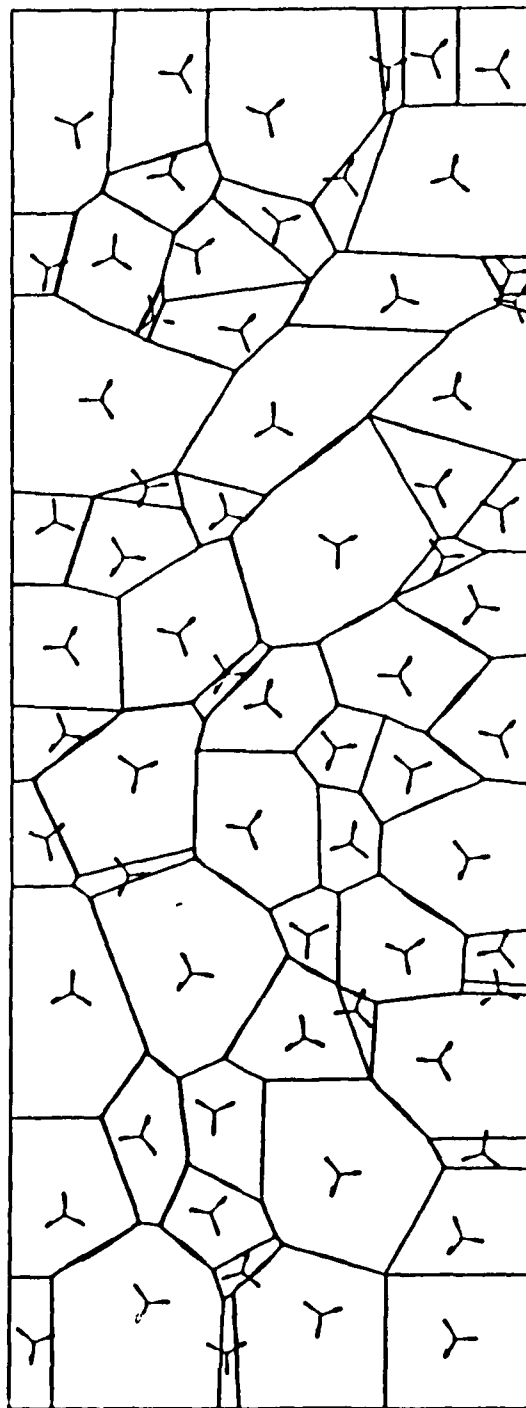


Figure 2 - Wide stripe A after equilibration

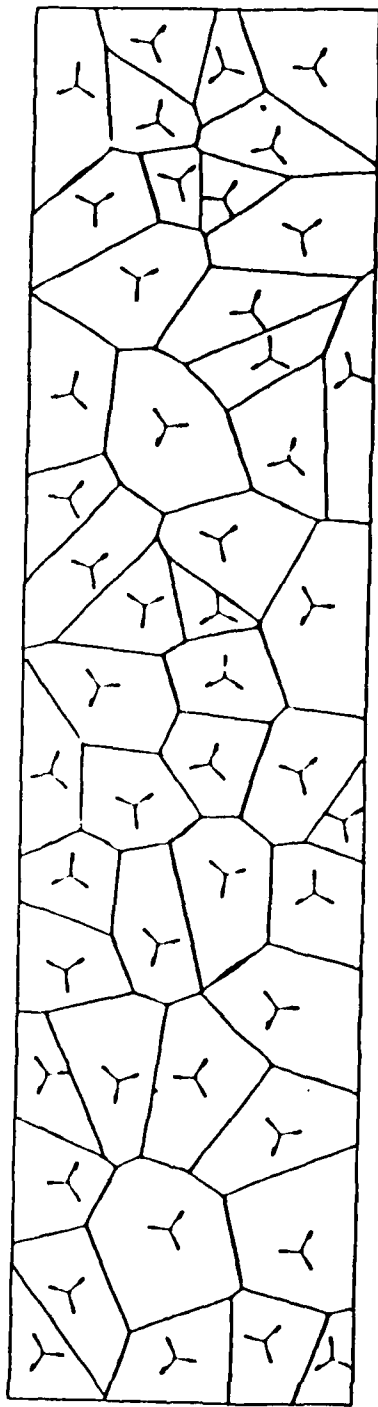


Figure 3 - Stripe B - Voronoi construction

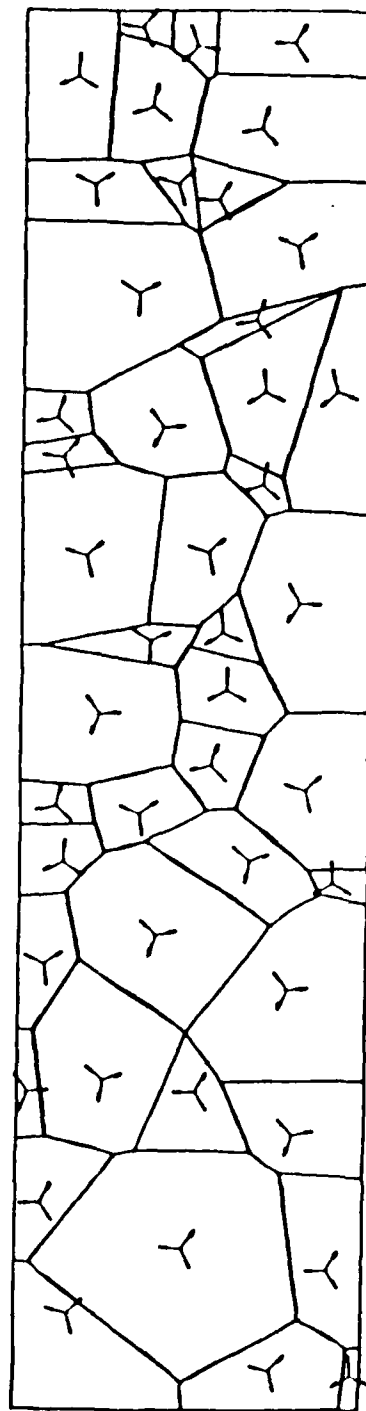


Figure 4 - Stripe B after equilibration

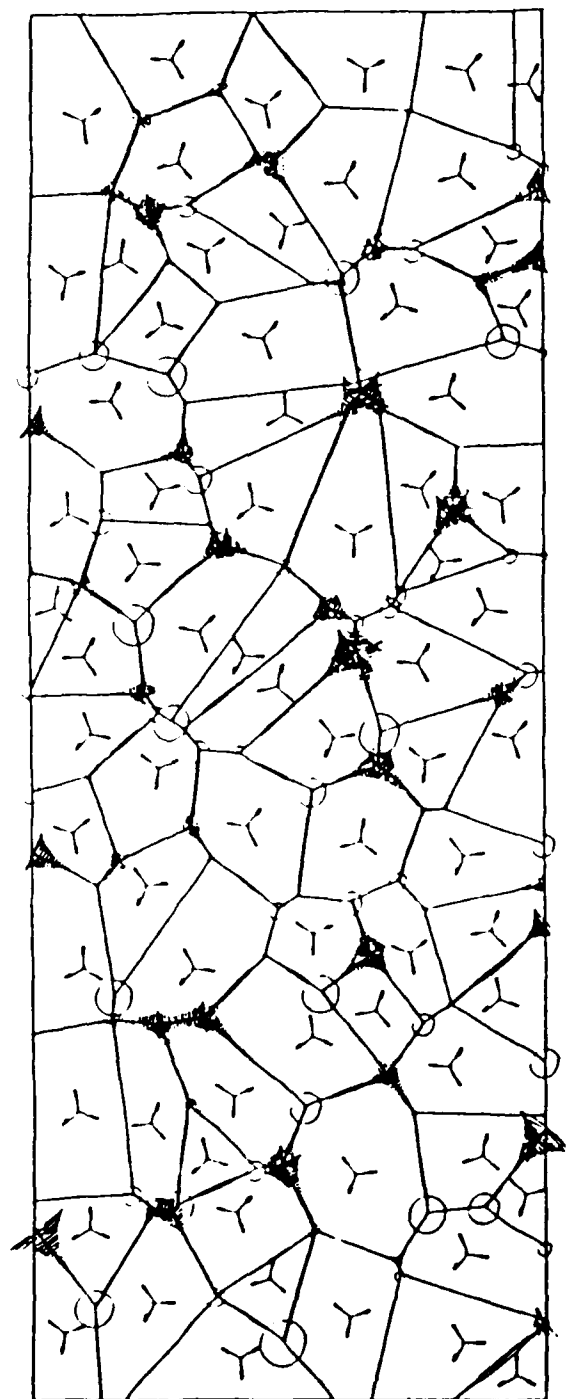


Figure 5 - Effect of electromigration on Stripe A - before equilibration

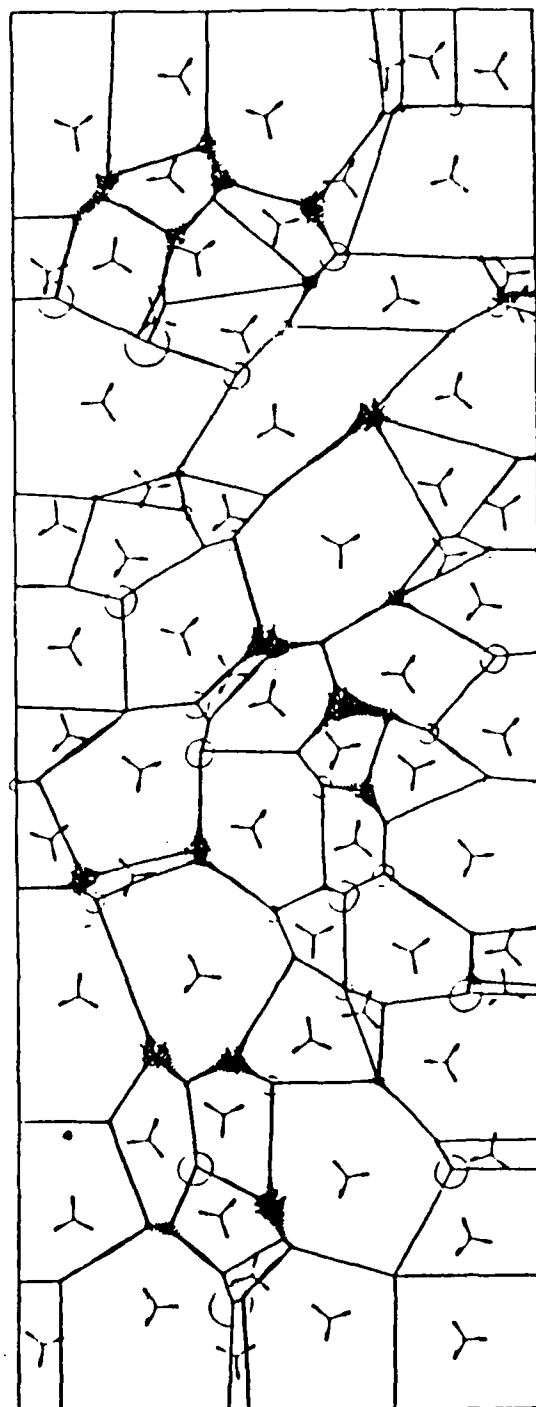


Figure 6 - Effect of electromigration on Stripe A - after equilibration

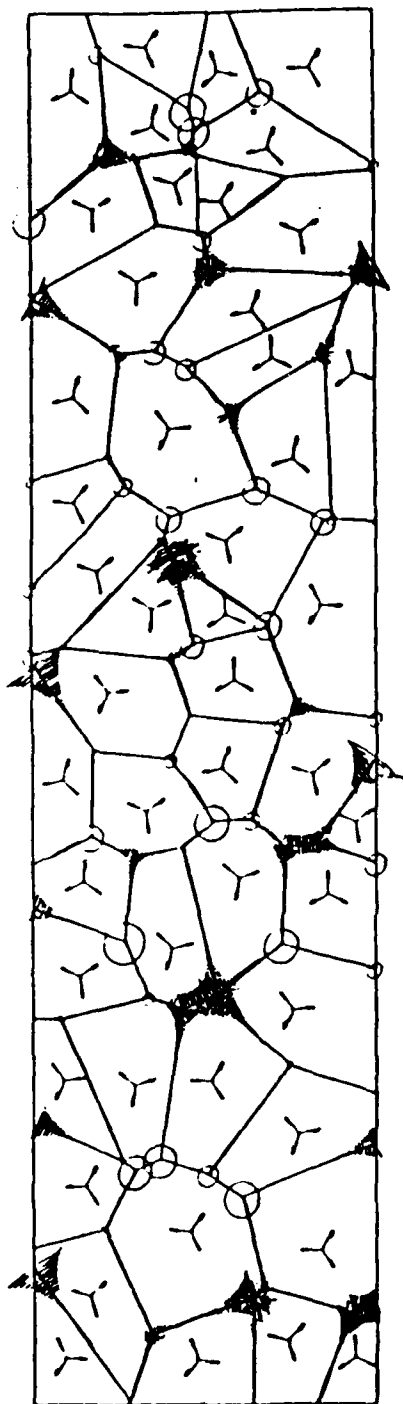


Figure 7 - Electromigration on Stripe B - before equilibration

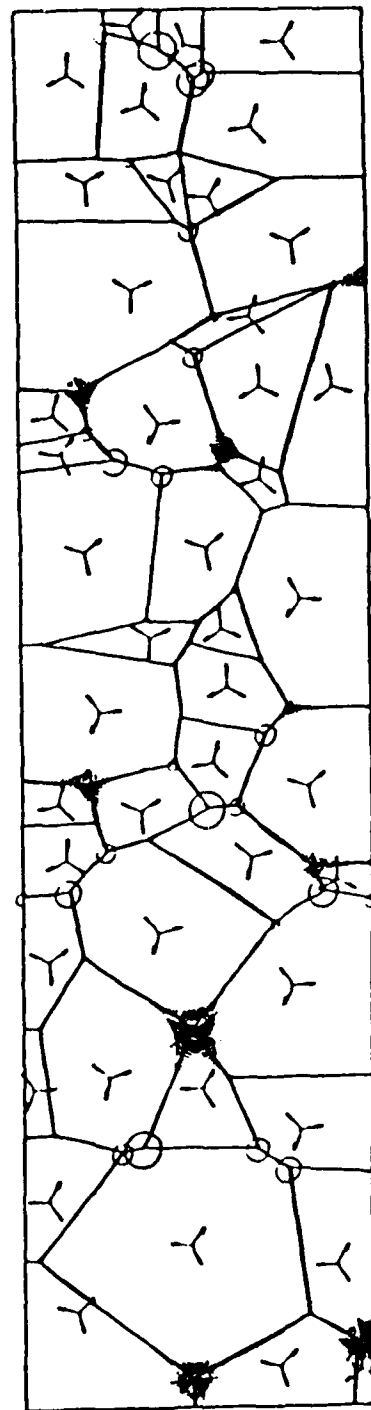


Figure 8 - Electromigration on Stripe B - after equilibration